Welding Procedures Specification for Flux Cored Arc Welding of Wind Towers

By Nelson da Cunha de Matos, Instituto Superior Técnico

Abstract

The main objective of the study concerns the development of a welding procedure using flux cored wire in order to allow a new design concept for large wind energy towers with increased base diameters. The innovation of this concept is the replacement of ring flanges by onsite welds which improves the fatigue resistance, enables the introduction of higher steel grades and erection of wind energy converters (WEC) in remote areas with limited accessibility.

Welding trials and preparation of Welding Procedure Specifications Flux Cored Arc Welding (FCAW) tests were carried out, a wide selection of self-shielded and gas-shielded wires were tested and evaluated for their overall weldability, especially. In the vertical-up position, since it is the most relevant for FCAW during the erection of the tower.

Welded samples in S355J2 and S460M steel were subjected to mechanical tests and micro-structural analysis in order to ascertain their suitability for the efforts expected in a WEC.

Introduction

Due to environmental constraints greenhouse gas emissions must be reduced according to the Kyoto Protocol[1] and new methods to gather energy with lower levels of pollution and to reduce the carbon footprint have been developed. The new technologies emerging from this effort are called Green Energy. [2]

Renewable technologies are essential contributors to sustainable energy as they generally contribute to world energy safety, reducing dependence on fossil fuel resources, and providing opportunities for mitigating greenhouse gases.

Leading the renewable technologies is wind energy conversion. Wind energy is an attractive alternative to fossil fuels mainly because is a clean, renewable, plentiful and widely distributed source of energy.

Nowadays, conventional WEC towers have reached road transportation limits in dimension and weight. Limited accessibility conditions of onshore remote areas, where best wind conditions exist, do not permit the installation of larger and more efficient WEC. This requires transport of parts, assembly and erection on site.

This study targeted the ability to use mechanized Flux Cored Arc Welding (FCAW) to connect tower sections onsite made with S355J2 and S460M steels maintaining mechanical properties required for this type of construction.

Manual and mechanized trials were performed in S355J2 and S460M steels using self-shielded and gas-shielded wires.

All welded samples were visual inspected and submitted to Radiographic and Ultrasonic testing according to ISO5817.

WEC innovation

Replacing Submerged Arc Welding done in factory by mechanized FCAW onsite and using higher steel grades such as S460M will enable onsite manufacturing of the lower tower sections in a mobile factory overcoming transportation restrictions and allowing larger bottom diameters and thinner walls. By allowing larger diameters and having a lighter structure total WEC height, weight of the nacelle and rotor can be increased and in consequence energy conversion efficiency will also increase.

Another positive feature, of this alternate means of manufacture, is the expected improved fatigue behavior due to the replacement of bolted connections by welding.

FCAW characteristics

Flux Cored Arc Welding has developed significantly since 1950, having overcome many of the restrictions associated with Shielded Metal Arc Welding and becoming a competing technology of Gas Metal Arc Welding. FCAW was developed primarily for welding thick and out-of-position structural steels both in closed shop environment and outdoors.

For this study self-shielded wires are of particular interest since all welding work shall occur outdoor at the mercy of nature. This type of wire does not require externally supplied protection gas for shielding, unlike gas-shielded wires, vaporization and decomposition of core ingredients provide protection to the weld creating their own shielding gas.

Gas-shielded wires are easier to work with, and do not require such an accurate technique as with self-shielded, however if used in a windy environment without any additional protection of the welding area the loss of protection of the gas from air flow can lead to weld imperfection namely porosity.

Experimental procedure

The main purpose of this work was guarantee a mechanized FCAW alternative to SAW providing defect-free welds and mechanical properties required for WEC towers.

The trials were divided in four stages. In the first stage the most appropriate filler wire was selected to the task at hand, which was welding vertical up joints. The wire with best results in welding parameters optimization was then used for the remaining trials.

The parameters to be studied and optimized were: Wire feed speed, current, arc voltage, stickout, travel speed, torch angle and weaving frequency / trajectory.

The wires tested in selection trials differentiated themselves by shielding/gas type, diameter and mechanical properties. Chosen wires for selection trials

Self-Shielded: Lincoln Electric NR-233 (1.6mm); NR203Ni1(2.0mm);NR-Offshore(2.0mm); ESAB Coreshield 8(1.6mm); Coreshield 8 Ni1 H5(1.6mm)

Gas-Shielded: ESAB PZ6113(1.2mm); PZ6113S(1.2mm); PZ6114S(1.2mm); PZ6116S(1.2mm); PZ6138(1.2mm)

For the selected wire a Preliminary Specification of Welding Procedures was defined for the 10mm and 30mm thickness joints. The second stage was initiated after obtaining a satisfactory welding procedure. Microstructural properties analysis and hardness tests were conducted on S460M steel for different heat input (HI).

In the third step fully mechanized welding trials were performed on smaller sample test pieces to check the welding settings. Non Destructive Testing (NDT) such as Ultrasonic and Radiographic testing were used to assess the existence of any welding imperfection.

In the last trial all knowledge from the previous trials was used to produce flawless test pieces that later underwent to confirm mechanical properties required.

Results

1. First trial

Best results of the first trial were obtained with NR-203Ni1 and PZ6113S self-shielded and gas-shielded type respectively.

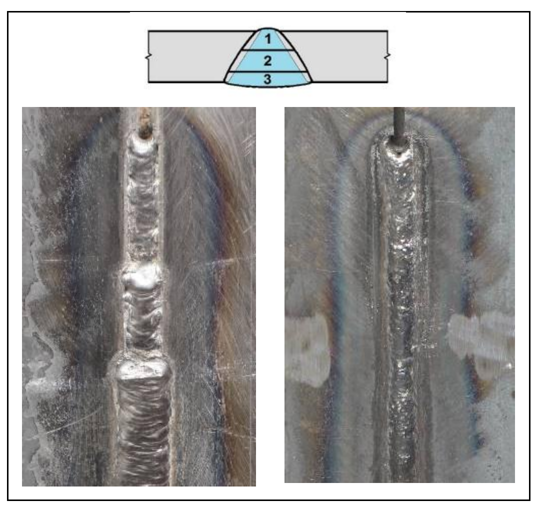

Figure 1 - Example of a semi-automatic welding joint using a self-shielded wire (NR-203Ni1.Left: front side of welded joint; right: back side of welded joint.

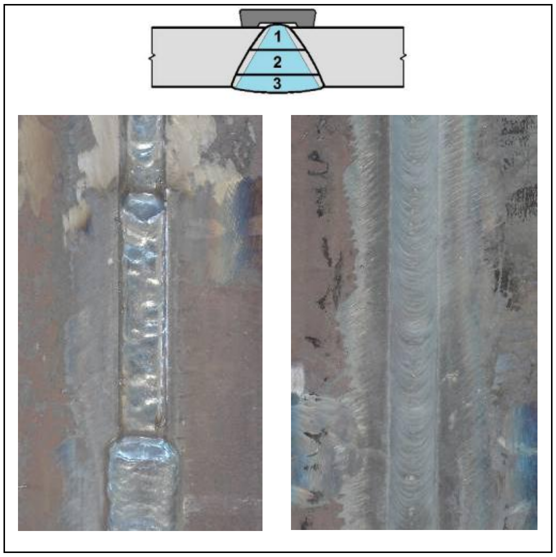

Figure 2 - Example of a semi-automatic welding joint using a gas-shielded wire (PZ6113S): Left: front side of welded joint; right: back side of welded joint.

Wire	Deposition rate (Kg/h)	
	Root	Fill & Cap
NR233	1,6	2,3
NR203Ni1	1,4	1,7
NR Offshore	1,3	1,7
Coreshield 8	1,4	1,4
Coreshield 8 Ni1	1,1	1,6
PZ6113	2,1	3,2
PZ6113S	2,1	3,2
PZ6114S	2,1	3,2
PZ6116S	2,1	3,2
PZ6138	2,1	3,2

Table 1 - Deposition rate of all tested wires.

From visual inspections, deposit rates and overall weldability the best wire tested was PZ6113S.

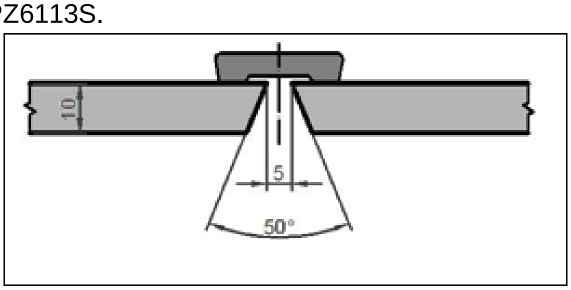

Pass no.	Wire feed speed	Voltage	Current (typical)	Weld speed	Heat input	Deposition rate
	[m/min]	[V]	[A]	[cm/min]	[kJ/mm]	[kg/h]
1	6.0	23	160	11	2.0	2.1
2, 3	8.0	25	190	18	1.7	2.8

Figure 3 - Welding joints (10mm), sequences and parameters for vertical-up (PF) position with PZ6113S.

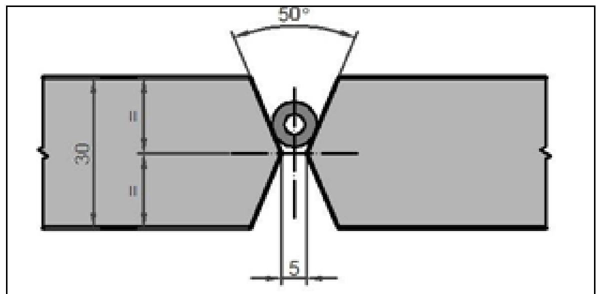

Pass no.	Wire feed speed	Voltage	Current (typical)	Weld speed	Heat input	Deposition rate
	[m/min]	[V]	[A]	[cm/min]	[kJ/mm]	[kg/h]
1	6.0	23	160	10	2.2	2.1
2-8	9.0	27	210	17	2.0	3.2

Figure 4 - Welding joints (30mm), sequences and parameters for vertical-up (PF) position with PZ6113S.

2. Second trial

With all the objectives and results of the first test completed the second trial began by obtaining the desired heat input with two different approaches. The first approach combined different values of wire feed speed (WFS) with welding speed (WS), This was used for test specimens from A to G, the remaining specimens were welded with the other approach consisted on maintaining the WFS value constant and varying only the WS.

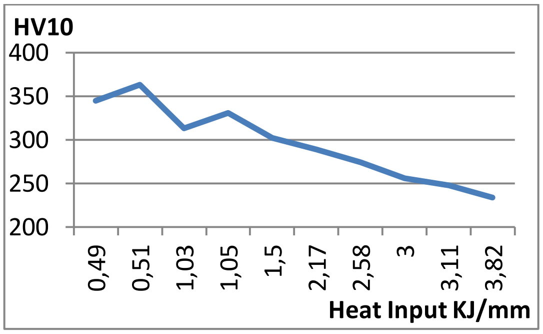

Figure 5 - Maximum Hardness for each heat input value tested.

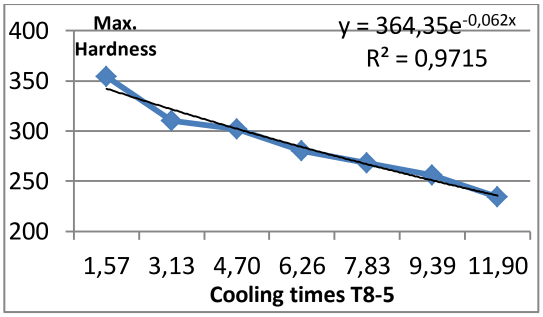

Figure 6 - Max. hardness relation with cooling times obtained with Rosenthal analytical solution.

All specimens presented acicular ferrite, polygonal ferrite, in the weld material, in the low heat input specimens some formations of martensite, and bainite were detected. The unaffected parent material presented ferritic and perlitic structures.

Microstructural differences were best seen in the heat affected zone as it was expected. Specimens with lower heat input (A, B, C, H, I) have martensitic and bainite structures in the grain growth and in the refined grain areas as well. Traces of perlite and some aggregated carbides are present in the subcritical region. In the specimens with Hi higher than 2.5KJ the grain growth region has ferrite with aligned M-A-C and ferrite carbide aggregates, in the subcritical region ferrite and spheroidized pearlite are present.

3. Third trial

The first and second trials gave the opportunity to initiate mechanized welding with well-defined parameter boundaries. Few changes were needed to achieve sound welding beads with good penetration and morphology. One parameter of paramount importance is the angle of the torch in all passes but especially on root and cap passes, by controlling the torch angle a good penetration or fill can be obtained. For root passes it was found that a downward angle, about 15º with horizontal plane, provided the correct amount of penetration and good joint filling.

For cap passes the decision of what angle was more appropriate was difficult because not only the welding speed and torch angle influenced the cap but also weaving frequency and amplitude.

The preferred angle for fill and cap pass was an angle of 0º with horizontal plane, with a 0.2 seconds dwelling right and left with a frequency of 1Hz, as for the width of the weaving was normally 2mm shorter than the gap of the joint in the actual pass.

Mechanized test pieces were subjected to ultrasonic testing and if any imperfection was detected welding parameters and procedures were refined until flawless welding bead was achieved.

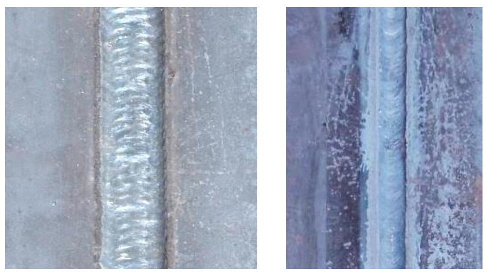

Figure 7 - Completed welding joint. Left: front side, right: back side of welded joint.

Most problematic imperfection found was porosity. Welding parameters and conditions were check and arrived at the conclusion that that the cause was incorrect gas flow rate. By consulting gas flow efficiency information in " Wilkinson, M. E., Direct Gas Shield Analysis to Determine Shielding Efficiency. Report of The Welding Institute (TWI), Cambridge, England;" and applying, the *Reynolds* number (Re) from fluid mechanics, a flow line was plotted which facilitated the establishment of a new and more efficient flow rate however the exact transition will be dependent on the diameter of torch used, this study provided some perspective and cautions on the use of too high a flow rate.

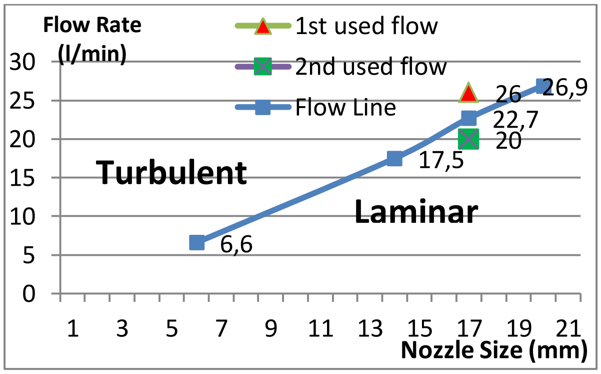

Figure 8 - Shielding gas flow regions.

4. Fourth trial

Similarly to the third trial mechanized samples with no imperfections were welded with the purpose of being submitted to mechanical tests.

Even with all the trials done before and welding procedure well established some imperfections were detected in some samples. In twenty nine samples four showed presence of imperfections such as intermittent undercut, slag inclusions and gas pores.

Three test pieces, despite the imperfections found, are classified by ISO 5817 as class B (highest quality level). Only one test piece had imperfections not permitted by the standard, none of the other three test pieces with imperfections required repair.

The case of the test piece with not acceptable is present below.

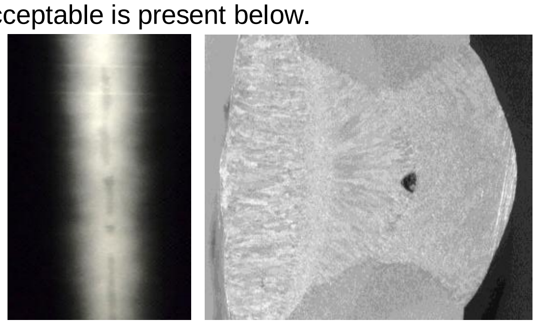

Figure 9 – Welding Imperfection Radiography parameters of ST005, 170mm to 335mm; Macrograph of ST005 weld bead showing a slag channel

The defect was a slag inclusion.

After evaluating the defect the most probable cause found for this to happen was due to the method of removing the root slag.

There are two hypotheses to explain the slag inclusion:

1- The cut made by the grinder entrapped slag in the small groove of the cut and the second pass did not melted adequately the root pass leaving slag embedded in the bead.

2- The cut originated a small groove that was enough to entrap the slag of the second pass by disturbing the weld flow.

Not being sure which one was the defect cause, slag removal procedure and welding procedures were altered in order to eliminate all possible causes. Conventional slag cut was made on left and on right instead of being centered, the cut did not touch the weld bead. Welding speeds were increased in order to avoid a cushion effect and provide a better penetration by the arc travelling on the edge of the molten material.

After all welds quality was confirmed by ultrasonic and radiographic testing, Charpy and tensile tests were also carried out on several test pieces.

Test Reference	Yield Strength Mpa	Tensile Strength MPa	Elongation after fracture %
ST004_T1	531	614	25,3
ST004_T2	540	650	27,1
ST004_T3	610	695	27,7
ST006_T1	476	596	29,0
ST006_T2	524	644	26,2
ST006_T3	496	599	24,8
ST013_T1	552	680	27,5
ST013_T2	559	699	27,4
ST013_T3	558	715	29,9
ST020_T1	495	625	28,1
ST020_T2	516	632	28,8
ST020_T3	536	664	27,6

Table 2 – Tensile test results

ST013 & ST014				
Temp. (ºC)	Weld Metal	Fusion Line	FL+2mm	FL+5mm
22	91	67	48	56
-20	69	60	28	40
-50	47	20	19	17

Table 3 – Charpy test

Analysis of results

Filler wire selection

Self-shielded wires seemed to have good potential for application in the scope of the project. These wires were valid choices as they are all-position wires for structural welding of mild and some alloy steels but also suitable for single- and multi-pass welding however self-shielded wires were not capable of matching mechanical properties of S460M steel.

All gas-shielded filler materials that have been tested are 1.2mm diameter all-position rutile wires which differ among them mainly on nickel content and corresponding toughness properties of the weld metal. All gas-protected rutile flux-cored wires tested, PZ6113 (with Ar/CO_2), PZ6113S, PZ6114S, PZ6116S and PZ6138, all match entirely the properties of S460M steel.

Not only gas-shielded wires are capable of a much better overall weldability but also have deposition rates notoriously higher than their self-shielded counterparts.

It is known that as the cross sectional area of a conductor decreases, the resistance to current flow increases. This resistance to current flow will cause considerable heating of the conductor if the current is relatively high and the conductor is small in cross sectional area. In other words, at a given current in amperes, the current density within the conductor will increase as the diameter of the conductor is reduced.

It is this high current density that makes flux cored wires the success they are. The high resistance heating of the wire is confined to a small area, and the electrode reaches its' melting point very quickly, producing a concentrated deep penetrating arc. The deposition rate and the efficiency are very high.

The current density is considerably higher in the small diameter flux cored wire and therefore the deposition rate will also be somewhat higher. For example the smallest self-shielded (SS) wire tested was 1.6mm and gas-shielded (GS) was 1.2mm, the resistive area of SS is 77% bigger than GS and even increasing the stickout length to its limit it was proven impossible to compensate the resistance difference, as it can be seen in Table1 were the best SS wire has a deposition rate of about 75% of any GS.

To match GS wires performance SS wires must increase its welding current however the only parameter which increases the current besides stickout (which is limited) is wire feed speed that also has a limit. More current implies hotter molten metal and more wire fed, in these conditions it is impossible to the molten metal solidify quickly enough to sustain the following metal deposited by the weaving motion.

Pure carbon dioxide is not an inert gas because the heat of the arc breaks down the CO_2 into carbon monoxide and free oxygen. The use of pure CO_2 as welding gas, instead of 20% CO_2 argon-based mixtures, results normally in lower values of hydrogen as CO_2 react at these high welding temperatures producing a hotter puddle than truly inert atmospheres. The thermal conductivity of the gas at arc temperatures influences the arc voltage as well as the thermal energy delivered to the weld. As thermal conductivity increases, greater welding voltage is necessary to sustain the arc. For example, the thermal conductivity of helium and CO_2 is much higher than that of argon, because of this they deliver more heat to the weld. As result the use of CO_2 improves the molten puddle flow characteristics and hydrogen diffusion, since the elevated solubility of hydrogen allows hydrogen to diffuse out of the metal while this is at elevated temperatures.

In spite of the need to provide protection from wind in the immediate vicinity of the welding area, gas-shielded wires are strongly recommended for mechanized FCAW applications within the scope of the project, the final choice of FCAW filler material fell on PZ6113S due to lower cost related to welding (gas type) and very similar properties with the remaining PZ wires.

S460M Weldability Test

The microstructural changes between different heat input samples can be explained by the cooling time. A high heat input will result in a slow cooling rate, for a carbon steel, a slow cooling time over the temperature range of 800 to 500º C, results in a predominantly ferrite and pearlite microstructure.

A low heat input will result in a high cooling rate. A fast cooling time over the temperature range of 800 to 500º C, results in a predominantly ferrite and equal quantities of bainite and pearlite in the microstructure.

Martensite is rare in weldments with 0.1 to 0.25% C and 1.0 to 2.0% Mn carbon steel welded with suitable fillers, a cooling time of less than 1 second over the temperature range of 800 to 500º C would be necessary to form martensite.

The application of Rosenthal analytical solutions for this kind of experimental work is always a rough approximation to real welding conditions, however with the necessary precautions when analyzing the data obtained some conclusions can be associated with the real case.

The predicted range of cooling times for a 0.5 kJ/mm weld sample was found to be around 1.6s, this translates to mean cooling rates of approximately 192ºC/s. On the opposite for a heat input of 3.8KJ/mm the cooling time increased to 12s and the cooling rate was about 25°C/s.

In Figure 6 the maximum hardness versus cooling times were plotted and a trend lines was added using an exponential equation, this trend line has a R^2=0.9715 which is a fairly good accuracy to the values plotted.

$$Max\ Hardness = 364{,}35e^{-0{,}062(Cooling\ time(s))}$$

This equation can be used to back track from a hardness value desired up to the HI necessary to achieve it.

With cooling times less than 4.7s there is a high probability to find martensite on the weld metal and also on the HAZ, these hard microstructures are above de 300HV since the supersaturated solid solution of carbon and alpha ferrite are not maintained between 800 and 500ºC have enough time to promote the grain growth and carbon diffusion.

Test pieces C, D and M had cooling times between 5 and 9s, this higher cooling time translated in the complete microstructural transformation of the weld metal in acicular and polygonal ferrite and long enough cooling time to transform austenite in bainite, avoiding martensite, in the HAZ.

For the remaining test pieces, G and N, with cooling time, above 9s, allowed the attainment of ferrite and spheroidized perlite in the subcritical zone very similar with the parent material whilst in the grain growth zone was identified ferrite with aligned M-A-C.

Consulting the standard ISO TR 15608 – 2005 the steel S460M belongs to the group 2.1 as it is a thermomechanically treated fine-grain steel with a specified minimum yield strength 360 /mm^2 < *R*eH ≤460 /mm^2 and consulting ISO 15614-1 2004 section 7.4.6 Table 2 the maximum permitted hardness value (HV10) for this type of joint and steel group cannot exceed 380HV10.

Even with the lowest heat input the maximum HV value obtained was 363 therefore according to the standards any of the welding parameters used are acceptable, however lower values of hardness ensure a less brittle structure and HI higher than 1.5KJ/mm should be used to safeguard a more ductile fracture.

As expected test pieces with lowest HI such as A, B, E,I with microstructures rich in bainite and martensite which has limited slip possibilities and a high yield strength, these test pieces also show higher hardness and brittleness in WM up to refined grain growth than all the others test pieces. The other test pieces with higher HI and slower cooling rates have small amount of polygonal ferrite and acicular ferrite, characterized by needle shaped crystallites with chaotic ordering, in the WM which confers a more ductile microstructure than martensite. Ferrite with aligned M-A-C was also found and although this kind of microstructures is not beneficial due to the presence of martensite and carbides which contribute to the embrittlement, hardness values were very alike to test pieces without this type of microstructures which leads to think that there is only a small amount of M-A-C.

It was also found that for same values of heat input obtained by higher wire feed speed result in slight lower values of hardness. This can be seen in Figure 5 where hardness values of 0.49 KJ/mm and 1.03KJ/mm, respectively test pieces H and I welded at 9cm/min, were 20HV10 lower than when the two test pieces welded at 6cm/min. One reason for this to happen is the cushion effect, at a slower welding speed the arc force is damped by the extra weld metal deposited this translate to a lower heat transmission to the piece as heat is partly dispersed by the weld bead itself, although the heat input is equal. As seen before lower temperatures are accompanied by higher cooling rates which lead to harder structures.

Mechanized welding trials

It was decided maintain constant the wire feed speed, therefore torch alignment, stick-out, welding speed and torch angle would be adjusted in order to compensate changes in joint geometry. The parameters obtained from the manual testing were very accurate working as guide lines needing just some corrections case by case as it is impossible to guarantee identical joint geometry of every test pieces and the mechanized system does not compensate unforeseen situations like a skilled technician does.

The most delicate and troublesome pass was the cap, not only because it was the surface one but also because it was the transitions from a weld bead starting within the joint and ending on the surface of the test piece.

Shielding gas flow rate is often a neglected factor in FCAW, the assumption that more gas flow results in better protection is misleading.

High gas flow surge at weld start causes turbulence in the shielding gas stream. This turbulence causes air to be mixed into the shielding gas stream until the flow rate stabilizes to the preset level. This entrained air causes, in addition to wasting shielding gas, excess weld spatter and can cause internal weld porosity. The gas flow required to efficiently protect the molten puddle cam be directly related to the welding gun nozzle size and distance to work piece First flow rate value used, which lead to some porosity, is marked as a red triangle in Figure 8. As can be seen it was not an excessive value however for the gas type and nozzle size being used it was too much. After plotting a flow line that separates approximately the turbulent regime from the laminar a new and conservative flow rate was tested, marked in the graph with a green square, with this new value the incidence of porosities cause by inadequate gas flow rate dropped to virtually zero.

In PA position with 10mm thickness was found to be impossible to make the root pass with welding speed higher than 7cm/min as the electric arc overtakes the molten bath and begins to unsettle. Same scenario was found in PF position with the welding speed limit being 11cm/min.

Mechanized welding samples

Although some defects were detected in the ST samples, according to ISO 5817, no repair was mandatory, except for one. The results obtained by NDT confirmed not only the quality of welded joints but also the ability to detect any kind of imperfection.

Methodology and welding parameters were very alike with the ones used in the mechanized trials and in twenty nine test pieces only one failed the standard requirements this shows that the welding procedure is robust and easily repeatable with high quality welds.

The major imperfection found on ST005 reveals that the welding position PA is more prone to develop this kind of imperfection than the PF position, this is related to the less efficient convection in the molten pool when welding in PA making any failure in the joint preparation is a possible triggering defect. The key to eliminate the imperfection was the homogeneous preparation of the joint to receive the second pass as it is nearly impossible to control weld flow conditions.

The disturbance of the weld flow can be explained by two types of flow generated.

The surface temperature of the weld pool will usually be maximum in the center of the weld pool and decreases with increasing distance from the center creating a temperature gradient which in turn will generate a surface tension gradient. The negative gradient of the surface tension generates outward directed flow called Marangoni flow (Figure 10), on the opposite side is the Lorentz flow (Figure 11) which generates electromagnetic forces in the weld pool due to divergency of the electric current causing pressure differences and resulting in downward directed flow.

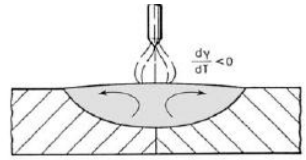

Figure 10- Marangoni flow

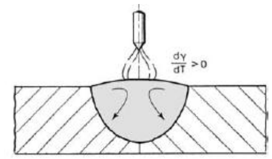

Figure 11- Lorentz flow

As result of these reversals, undesirable variations in penetration depth can occur and the existence of the small groove can be enough to produce the imperfection above described.

Tensile test results confirm the mechanical properties expected when welding with the chosen wire and these types of steel, the lowest value of yield strength registered was 476MPa above minimum value in the wire certificate as well in the steel certificate.

The values for these properties vary even between specimens of the same test sample, the maximum variation is about 81 MPa and this can be explained by some changes in the welding parameters to compensate inhomogeneous joint zones. These changes modify the heat input and joint filling, this can originate different microstructures consequently different mechanical properties. Ductility can be assessed by the other two parameter, area reduction and elongation after fracture. A material that experiences very little or no plastic deformation upon fracture is termed brittle and the converse is also true. The minimum elongation belongs to S460M steel with a value of 17% from tensile test done the lowest of all specimens was 24.8%, regarding the values of reduction of area and using once again ISO6892-1 this type of fracture is considered ductile.

Charpy impact tests determine the amount of energy absorbed by a material during fracture. All results obtained while testing confirm the predicted behavior, supplied by the wire and steel manufacturers, at all temperatures including at -50ºC which is an extreme temperature for both steel and filler wire. All test pieces absorbed amounts of energy above the minimum value in the wire and steel certificate for all temperatures. One other aspect of Charpy results is the energy difference between longitudinal and transverse specimen. Generally in the longitudinal specimen the energy absorbed increases along the distance from the weld metal in other words FL+5 will absorb the most amount of energy of all the locations followed by FL+2 then FL and finally WM, on the other and the transverse specimen behaves in the opposite way and has generally lower values than the longitudinal one.

One explanation is that longitudinal test metal across the grain of steel and have higher notch toughness than transverse. Thermomechanically rolled material possess long grain boundaries in rolling direction and another reason for the anisotropy is the elongation of non-metallic inclusions like manganese sulphide. At high temperatures the sulphide inclusions are harder than the matrix material, but in the temperature regime of the thermomechanical treatment the inclusions are softer. During the rolling process they stretch in the rolling direction and elongate resulting in anisotropic toughness behavior as a consequent, the Charpy impact values in the transverse direction are usually inferior to those in the rolling direction.

Conclusions

Although self-shielded FCAW wires have evolved greatly they are still a step behind the gas-shielded wires Self-shielded wires seemed to have good potential for application in the scope of SAFETOWER as mobility being the best property however self-shielded FCAW wires do not match mechanical properties of S460M steel and presented a very harsh and difficult arc behavior translating into an additional difficulty when trying to mechanize the procedure

Gas-shielded surpassed in every way their self-shielded counterparts, with mechanical properties similar to S460M, better deposition rates, steady behavior on ceramic backing provided a good start point to mechanize.

Parameters found manually needed very few corrections when mechanized, nevertheless constant oversight of the welding procedure is mandatory. A good joint preparation minimizes the corrections during welding and reduces the probability of imperfections as shown above.

S460M weldability test demonstrated the steel behavior when subjected to certain heat inputs, results show arising of some detrimental structures like martensite and carbides but in small quantities and the hardness values show that even with very low HI, according to ISO standard, all welds are acceptable. However the use of HI equal or higher than 1.5KJ/mm will result in more favorable microstructures and so it is advisable.

The Rosenthal analytical solution applied to welding proved to be a fairly accurate tool to predict heat behavior in steel however have some attention must be taken when working with to intermediate thicknesses.

The NDT chosen to verify the weld quality will also be important for the future of the project, specially UT as it is safe to operate (no radiation emission) and fairly easy to mechanize, two very important properties since it is going to be operated on site. Weld quality was verify not only by NDT but also by mechanical testing such as tensile test and impact tests, that ensured structural integrity of welded joints. The values obtained by these tests were well within the acceptable range of the materials in question and for the use they are intended for.

The tensile and Charpy tests performed proved the mechanical qualities expected of this type of material and process and within the range recommended by ISO standards.

From this work it can be concluded that use of FCAW for onsite build and erection of WEC is a good substitute for the current method of fabrication and erection of WEC using bolted flanges. CTOD, high cycle fatigue, and bending tests are scheduled to be executed in the near future to complement the tests already done.

References

[1] UNFCC, 2007. Kyoto Protocol. [online] Available at: <http://unfccc.int/kyoto_protocol/items/2830.php> [14 July 2011]

[2] Jacobson, Mark Z. & Archer, Cristina L. ; Saturation wind power potential and its implications for wind energy 2012

[3] Marvel, Kate; Kravitz, Ben & Caldeira, Ken; Geophysical limits to global wind power 2012

[4] Staffan Engström, Tomas Lyrner, Manouchehr Hassanzadeh, Thomas Stalin and John Johansson, Tall towers for large wind turbines- Report from Vindforsk project V-342 Höga – July-2010

[5] AWS, Welding Processes Part 2, 9th Edition, Volume 3

[6] James F. Lincoln Arc Welding Foundation, 2000, The Procedure Handbook of Arc Welding, 14th Edition, Lincoln Electric

[7] Quintino, L.; Santos, J.; "*Processos de Soldadura"*, Instituto de Soldadura e Qualidade, 2.ª Edição, 1998

[8] Fernandes, Paulo Eduardo Alves; Evaluation of fracture toughness of the heat affected zone (HAZ) of API 5L X80 steel welded SMAW and FCAW. São Paulo,2011

[9] Anmol S. Birring, "Ultrasonic Testing in Electric Power Plants," *NDT Handbook, Ultrasonic Testing*, 3rd Edition, ASNT, 2007

[10] Mostafa ; M.N. Khajavi Optimization of welding parameters for weld penetration in FCAW 2006 Journal of Achievements in Materials and Manufacturing Engineering

[11] STARLING, Cícero Murta Diniz; MODENESI, Paulo J. and BORBA, Tadeu Messias Donizete. Bead characterization on FCAW welding of a rutilic tubular wire. *Soldag. insp. (Impr.)* [online]. 2009

[12] Krauss, G., 1992, "Heat Treatment and Processing Principles Materials Park" American Society for Metals.

[13] Doherty, R.D., Martin J.W. Cantor, B. 1997, "Stability of Microstructure in Metallic Systems".

[14] Smith, W. F., *Princípios de Ciência e Engenharia de Materiais*, 3ª Edição McGraw-Hill de Portugal, 1998

[15] Lopes Dias, E. M.; Miranda R. M.; "*Metalurgia da Soldadura"*; Instituto de Soldadura e Qualidade, 1993

[16] http://www.staff.ncl.ac.uk/s.j.bull/mmm211/PHASE/index.htm [6 December 2011]

[17] SADEK A ,IBRAHAM R N, PRICE J W H,SHEHATA T, USHIO M; Effect of Welding Parameters of FCAW Process and Shielding Gas Type on Weld Bead Geometry and Hardness Distribution. 2001

[18] Murray, Amanda. Examination of SAW and FCAW high strength steel weld metals for offshore structural applications Cranfield University Current Institution 1997